



Synthesis, antioxidant activity and SAR study of novel spiro-isatin-based Schiff bases

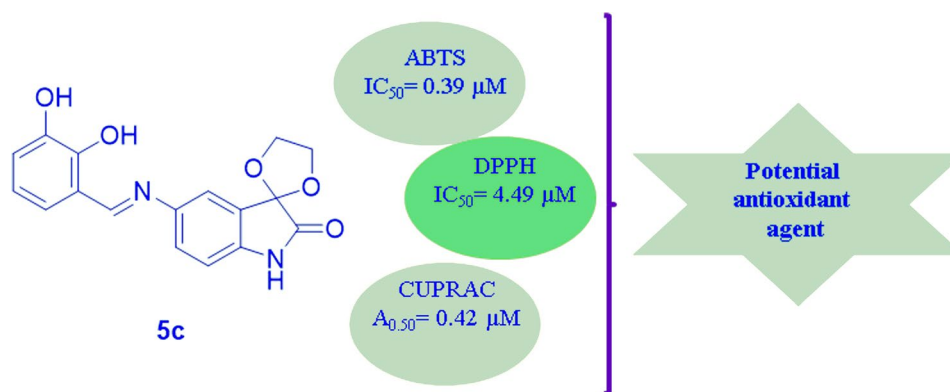
Fatih Sonmez¹ · Zuhale Gunesli¹ · Belma Zengin Kurt² · Isil Gazioglu³ · Davut Avci⁴ · Mustafa Kucukislamoglu⁵

Received: 22 September 2018 / Accepted: 13 December 2018
© Springer Nature Switzerland AG 2019

Abstract

A new series of 21 Schiff bases of spiro-isatin was synthesized, and their DPPH, CUPRAC and ABTS cation radical scavenging abilities were investigated for antioxidant activity. The results showed that all the synthesized compounds exhibited antioxidant activity for each assay. 5-(2,3-Dihydroxybenzylideneamino)spiro[[1,3] dioxolane-2,3-indoline]-2-on (**5c**) ($IC_{50}=4.49 \mu\text{M}$, for DPPH; $IC_{50}=0.39 \mu\text{M}$, for ABTS⁺; and $A_{0.50}=0.42 \mu\text{M}$, for CUPRAC) showed significantly better ABTS, CUPRAC and DPPH radical scavenging ability than quercetin ($IC_{50}=8.69 \mu\text{M}$, for DPPH; $IC_{50}=15.49 \mu\text{M}$, for ABTS⁺; and $A_{0.50}=18.47 \mu\text{M}$, for CUPRAC), which is used as a standard. SAR study showed that the synthesized compounds had higher ABTS⁺ activity than DPPH and CUPRAC activities. Moreover, the compounds (**5c** and **5d**), containing two hydroxyl groups, exhibited the highest antioxidant activities for all assays. Quantum chemical calculations were also carried out to support SAR results.

Graphical abstract



Keywords ABTS · Antioxidant activity · CUPRAC · DPPH · Isatin · Schiff base

Electronic supplementary material The online version of this article (<https://doi.org/10.1007/s11030-018-09910-7>) contains supplementary material, which is available to authorized users.

✉ Fatih Sonmez
fsonmez@sakarya.edu.tr

¹ Pamukova Vocational High School, Sakarya University of Applied Sciences, 54900 Sakarya, Turkey

² Department of Pharmaceutical Chemistry, Faculty of Pharmacy, Bezmialem Vakif University, 34093 Istanbul, Turkey

³ Department of Analytical Chemistry, Faculty of Pharmacy, Bezmialem Vakif University, 34093 Istanbul, Turkey

⁴ Department of Physics, Sakarya University, 54100 Sakarya, Turkey

⁵ Department of Chemistry, Sakarya University, 54100 Sakarya, Turkey

Introduction

Reactive oxygen species (ROS) play an important role in the formation of various serious diseases, such as cancer, heart diseases, diabetes, arteriosclerosis and cataracts. The harmful effects of free radicals that cause potential biological damage are called oxidative stress [1]. Free radicals in the human body play a pathogenic role in the formation of many chronic degenerative diseases such as cancer, autoimmune, inflammatory and cardiovascular neurodegenerative diseases [2–4]. Free radicals are one or more unpaired electron-donating molecules, and they have the short half-life, low stability and high chemical reactivity [5, 6]. These radicals arise naturally or due to some biological functions related to phagocytosis, regulation of cell proliferation, synthesis of substances and signalling between cells. Radicals damage lipids, proteins or DNA [7]. In order to protect the tissue from these damages, it is important that the free radicals are put into an ineffective state [8]. For this reason, antioxidants have been shown to play an important role in protecting people against many fatal diseases [9, 10]. Antioxidants (Fig. 1) are defined as substances that delay, inhibit or eliminate oxidative damage to a target molecule when present in low concentrations in food or in the body. The human body has developed various mechanisms against the oxidative stress by naturally producing antioxidants in situ (endogenous antioxidants) as well as by providing antioxidants through food (exogenous antioxidants) [11].

Isatin (1H-indole-2,3-dione) is an important chemical building block. In humans, it is also found as a metabolic by-product of adrenaline and also in tissues and fluids of

mammals at different concentrations [12]. Most of the isatin derivatives have shown a variety biological activities, such as antimicrobial [13], antioxidant [14], anticancer [15], MAO inhibitor [16], antibacterial [17], α -glucosidase inhibitor [18], and antitubulin agent [19]. The presence of the indole ring in the structure of anticancer drugs such as sunitinib causes this skeletal structure to be subject to many anticancer-related investigations [20–22]. The classic phenolic compounds, aromatic and heterocyclic amines having N–H bond functions showed antioxidant properties. It has also been reported that most of the isatin derivatives have potential antioxidant activity [23, 24], and the lactam ring of isatin is responsible for having free radical scavenging activity due to its N–H and C=O moieties [25, 26].

Schiff bases are another important class of organic compounds. It is also known that Schiff bases have various pharmacological activities, such as antibacterial, antifungal, anti-malarial, anti-inflammatory and antipyretic as well as their use as dyes, pigments, starting materials, organic synthesis intermediates, catalysts and polymer stabilizers. The imine group present in the Schiff bases is responsible for biological activities, and these activities can be modulated in general by modifying the substituent groups in the molecules. In addition, Schiff bases are known as excellent ligands because the imine groups, forming chelates with metal ions, show strong affinity to transition metal ions [27, 28].

In this study, on the basis of the reported evidences, new Schiff bases, containing spiro-isatin derivatives, which can show strong antioxidant activity, taking into account the known properties of isatin and Schiff bases, were synthesized. The antioxidant activities of the synthesized compounds were determined using three different methods (ABTS, CUPRAC and DPPH), and structure–activity relationships were examined in detail. The frontier molecular

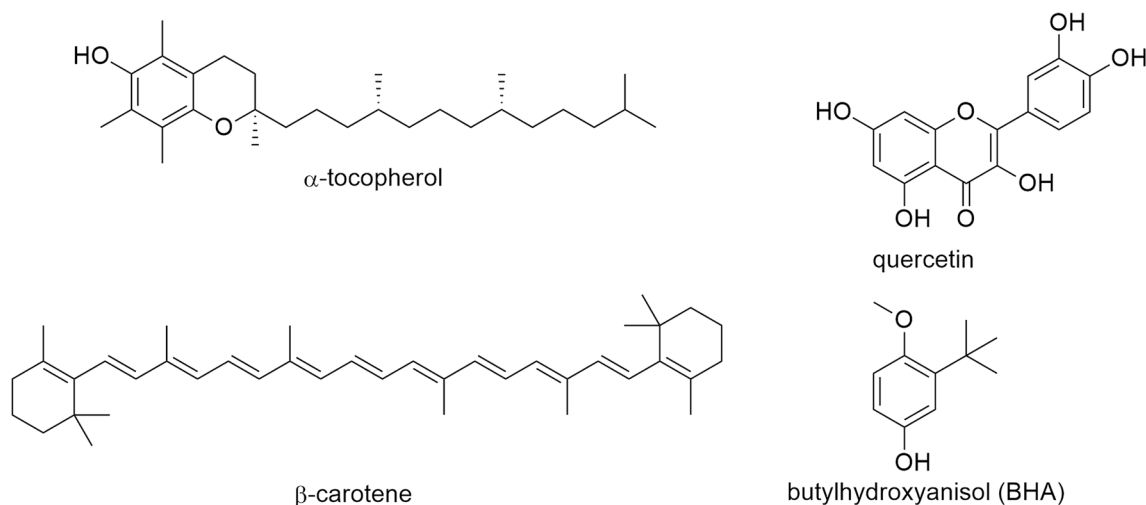


Fig. 1 The structures of some well-known antioxidant compounds

orbitals (FMOs) energies of the selected compounds were obtained by using the B3LYP/6-311G(d,p) level.

Results and discussion

Chemistry

The synthetic procedures employed to obtain the target compounds **5a–u** are depicted in Scheme 1. 5-Nitroisatin (**2**) was synthesized from isatin according to the literature [29]. Due to having high reactivity, the carbonyl group of isatin was protected with ethylene glycol [30]. The nitro moiety of 5-nitrospiro-isatin (**3**) was reduced with Pd/C, and 5-aminospiro-isatin (**4**) was reacted with different aldehyde derivatives to obtain Schiff base (**5a–u**) [31].

All the new compounds were characterized by ^1H NMR, ^{13}C NMR, IR, MS and elemental analysis. ^1H NMR, ^{13}C NMR, IR, MS of the **5a–t** are given in the Supplementary Materials. In the infrared spectra of the synthesized compounds, it was possible to observe the absorptions between 3140 and 3300 cm^{-1} relating to NH stretch for indole group, between 3350 and 3440 cm^{-1} relating to OH stretch for hydroxyl group, about 1520 cm^{-1} relating to C=N stretch for imine, absorptions in about 1700–1746 cm^{-1} from isatin carbonyl moiety stretch and absorptions between 1190 and 1230 cm^{-1} from acetal C–O moiety stretching. From the ^1H NMR spectra, the signal of proton NH at indole ring was between 10.50 and 10.65 ppm. The signals for aromatic hydrogens were observed between 6.70 and 7.90 ppm, and the signal of proton at imine group was detected about 8.60 ppm. The signals for aliphatic hydrogens were observed between 4.25 and 4.40 ppm. From the ^{13}C NMR spectra, the signals can be seen at 175 ppm, relating to isatin carbonyl moiety. This is followed by the sign about 159 ppm for imine carbon and about 90–150 ppm for aromatic carbons.

It is known that protecting by ethylene glycol is sensitive to pH value. Thus, in order to exhibit the diversity of spiro, the selected compound **5u** was mixed under the test condition (pH = 6.3 for ABTS and pH = 8.6 for DPPH). After that, ^1H and ^{13}C NMR of the products were acquired (Fig. 2). The presence of the signals of spiro moiety (at ~4.25 ppm for ^1H NMR and at ~66.3 ppm for ^{13}C NMR) confirms the structure is spiro-isatin derivatives not the isatin derivatives under the test conditions for ABTS and DPPH. It is not needed for CUPRAC assays due to carry out in neutral media (using $\text{NH}_4\text{CH}_3\text{COO}$ buffer, pH = 7).

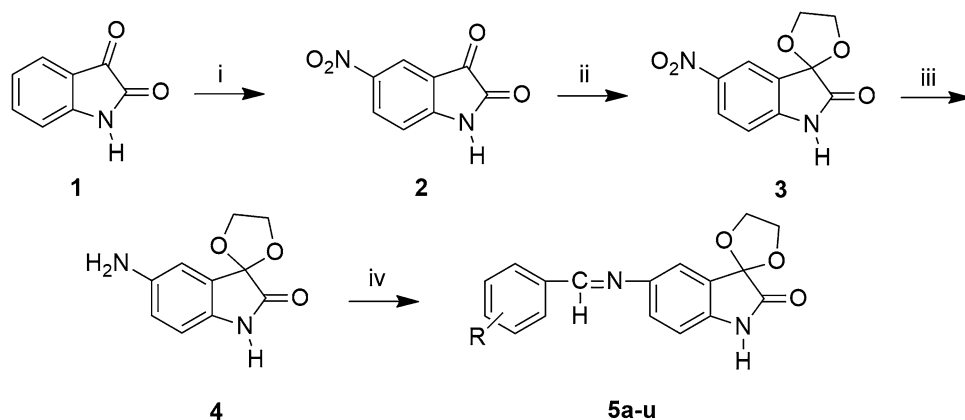
Antioxidant activity assay

It has been previously reported that antioxidant capacity determined by in vitro assays may differ from each other. Differences between DPPH and ABTS radical scavenging activities can be ascribed to reaction media. The DPPH assay is conventionally conducted under 50% ethanol/water, while the ABTS assay is carried out in aqueous conditions. Besides, compounds solubility in both media should be taken in consideration. Certain bioactive compounds may not soluble into reaction media and cannot express radical scavenging activities. Otherwise, the antioxidant capacities of the compounds depend on the mechanism of the assay. While the reaction runs on the cation radical in the ABTS assay, the reaction runs over free radical in the DPPH assay. In the CUPRAC assay, the antioxidant capacity depends on copper ion reduction power of the compound [32]. Consequently, in this study, these three different methods have been used for the determination of antioxidant capacity.

DPPH free radical scavenging assay

DPPH method is commonly used to measure the ability of antioxidants to sweep free radicals. In this spectrophotometric method, a stable free radical, DPPH

Scheme 1 Synthesis of new Schiff base-substituted spiro-isatin derivatives. Reaction conditions; (i) KNO_3 , H_2SO_4 , 2 h, rt; (ii) ethylene glycol, PTSA, benzene, 24 h, reflux; (iii) cyclohexene, 10% Pd-C, EtOH, 2 h, reflux; (iv) aldehyde derivatives, Et_3N , EtOH, 8 h, reflux



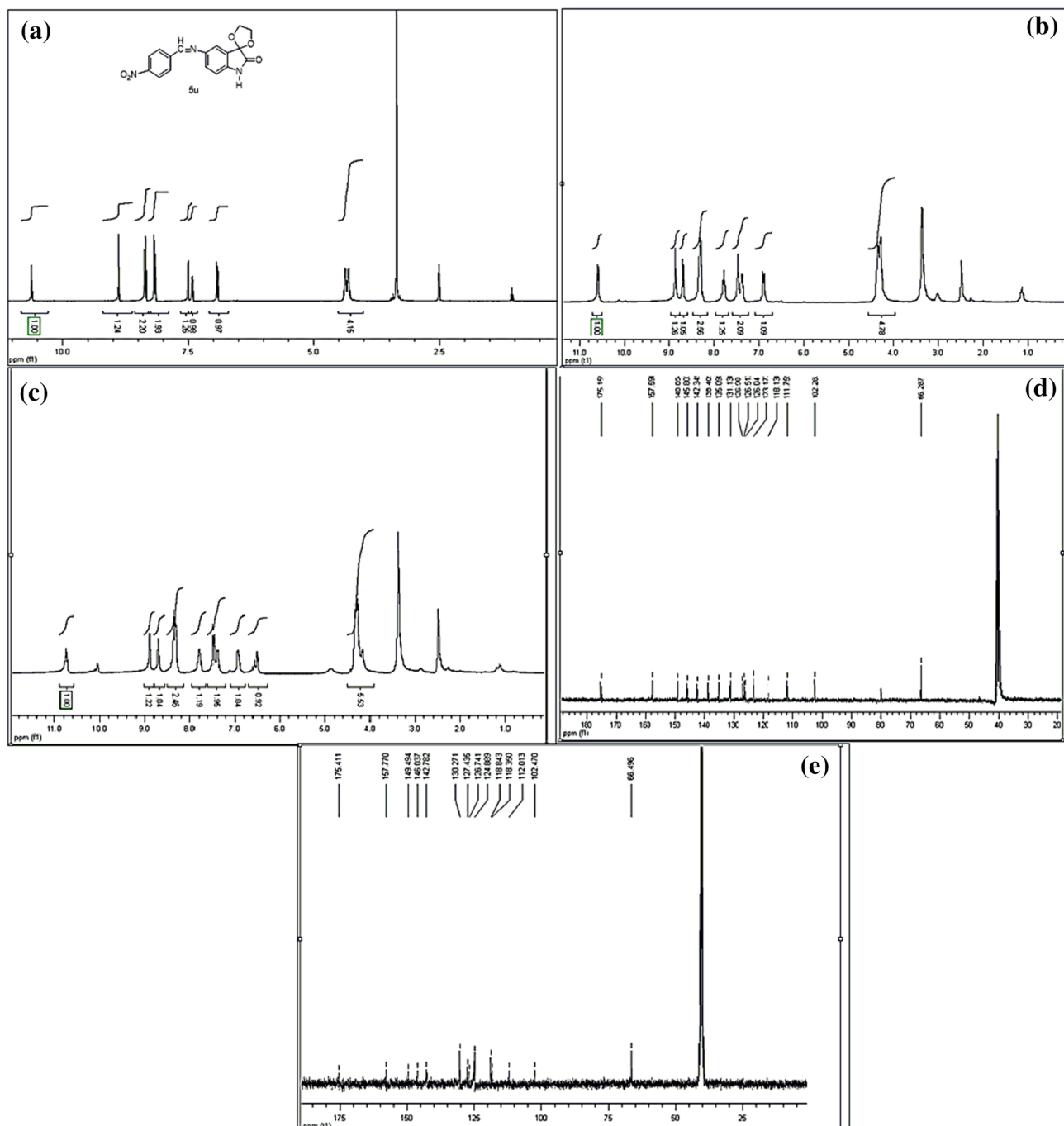
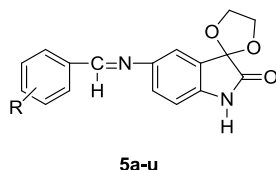


Fig. 2 **a** ^1H NMR of **5u** before antioxidant assay; **b** ^1H NMR of **5u** after mixing pH 6.3; **c** ^1H NMR of **5u** after mixing pH 8.6; **d** ^{13}C NMR of **5u** before antioxidant assay; **e** ^{13}C NMR of **5u** after mixing pH 6.3

(2,2-diphenyl-1-picrylhydrazyl), is used [33]. Antioxidants are based on the ability to degrade the DPPH radical, and when it interacts with radical hydrogen donors, hydrazine is reduced. According to this method, compounds must have strong hydrogen donor groups to exhibit good antioxidant properties. The IC_{50} values of the synthesized

compounds were between 4.49 μM and 204.90 μM for DPPH activity. Among them, only **5c** (IC_{50} = 4.49 μM) showed stronger antioxidant activity than quercetin (IC_{50} = 8.69 μM). Other compounds showed lower DPPH activity than quercetin (Table 1).

Table 1 IC₅₀ and A_{0.50} values (μM) of synthesized imine derivatives for antioxidant activities

| Compound | R | DPPH IC ₅₀ (μM) ^a | ABTS ⁺ IC ₅₀ (μM) ^a | CUPRAC A _{0.50} (μM) ^b |
|------------------|------------------------------------|--|---|---|
| 5a | H | 171.74 ± 1.24 | 18.45 ± 1.31 | 75.87 ± 0.04 |
| 5b | 3-OH | 94.81 ± 0.83 | 1.93 ± 0.33 | 18.76 ± 0.69 |
| 5c | 2,3-di-OH | 4.49 ± 0.45 | 0.39 ± 0.02 | 0.42 ± 0.02 |
| 5d | 2,5-di-OH | 18.65 ± 0.03 | 0.86 ± 0.03 | 1.35 ± 0.01 |
| 5e | 2,4,6-tri-OH | 64.03 ± 0.39 | 1.57 ± 0.05 | 12.99 ± 1.13 |
| 5f | 4-OCH ₃ | 145.00 ± 0.25 | 6.83 ± 0.84 | 28.74 ± 0.03 |
| 5g | 3,4-di-OCH ₃ | 130.00 ± 0.20 | 1.45 ± 0.28 | 28.06 ± 0.05 |
| 5h | 2,5-di-OCH ₃ | 81.78 ± 0.38 | 0.95 ± 0.01 | 17.59 ± 0.99 |
| 5i | 4-N(CH ₃) ₂ | 112.33 ± 2.49 | 1.56 ± 0.23 | 15.38 ± 0.38 |
| 5j | 2-F | 125.4 ± 0.63 | 1.25 ± 0.14 | 29.38 ± 0.02 |
| 5k | 3-F | 137.75 ± 2.67 | 1.06 ± 0.20 | 24.76 ± 0.38 |
| 5l | 4-F | 90.15 ± 0.59 | 0.98 ± 0.22 | 16.99 ± 1.47 |
| 5m | 2-Cl | 129.40 ± 0.46 | 2.43 ± 0.11 | 26.31 ± 0.05 |
| 5n | 3-Cl | 178.91 ± 0.37 | 1.48 ± 0.32 | 18.13 ± 1.56 |
| 5o | 4-Cl | 110.95 ± 0.72 | 1.28 ± 0.11 | 16.67 ± 0.40 |
| 5p | 2-Br | 143.90 ± 1.85 | 1.85 ± 0.23 | 20.92 ± 0.42 |
| 5q | 3-Br | 204.90 ± 3.52 | 1.45 ± 0.45 | 16.90 ± 0.68 |
| 5r | 4-Br | 127.16 ± 0.97 | 1.24 ± 0.14 | 16.15 ± 0.56 |
| 5s | 2-NO ₂ | 162.91 ± 0.98 | 19.2 ± 0.57 | 15.12 ± 0.23 |
| 5t | 3-NO ₂ | 126.62 ± 0.21 | 1.56 ± 0.46 | 19.23 ± 0.50 |
| 5u | 4-NO ₂ | 118.86 ± 0.68 | 1.38 ± 0.56 | 26.03 ± 0.04 |
| Quercetin | – | 8.69 ± 0.24 | 15.49 ± 2.33 | 18.47 ± 0.03 |

^aIC₅₀ values represent the mean ± SEM of three parallel measurements ($p < 0.05$)

^bA_{0.50} values represent the mean ± SEM of three parallel measurements ($p < 0.05$)

ABTS cation radical scavenging assay

The ABTS method is based on the ability of hydrogen or electron-donating antioxidants to decolorize the performed radical monocation of 2,2'-azino-bis(3-ethylbenzothiazoline-6-sulphonic acid) generated due to oxidation of ABTS with potassium persulfate [34]. The results indicated that the synthesized compounds exhibited good radical scavenging ability (Table 1.). IC₅₀ values of the synthesized compounds ranged from 0.39 μM to 18.45 μM for ABTS⁺ activity. They (except **5a** and **5s**) showed stronger antioxidant properties than the standard quercetin (IC₅₀ = 15.49 μM). Among them, **5c**, **5d**, **5h** and **5l** (IC₅₀ = 0.39, 0.86, 0.95 and 0.98 μM, respectively) showed significantly better activity than quercetin.

CUPRAC assay

As a distinct advantage over other electron-transfer-based assays (e.g. Folin, FRAP, ABTS, DPPH), CUPRAC is superior in regard to its realistic pH close to the physiological pH, favourable redox potential, accessibility and stability of reagents, and applicability to lipophilic antioxidants as well as hydrophilic ones. The cupric reducing antioxidant capacities of the synthesized compounds (**5a–u**) were determined according to the literature method [35] using quercetin as the standard compound. A_{0.50} values of the synthesized compounds were between 0.42 μM and 75.87 μM for CUPRAC activity. **5c**, **5d** and **5e** (A_{0.50} = 0.42, 1.35 and 12.99 μM, respectively) showed better cupric reducing antioxidant activity than quercetin (A_{0.50} = 18.47 μM). The others have

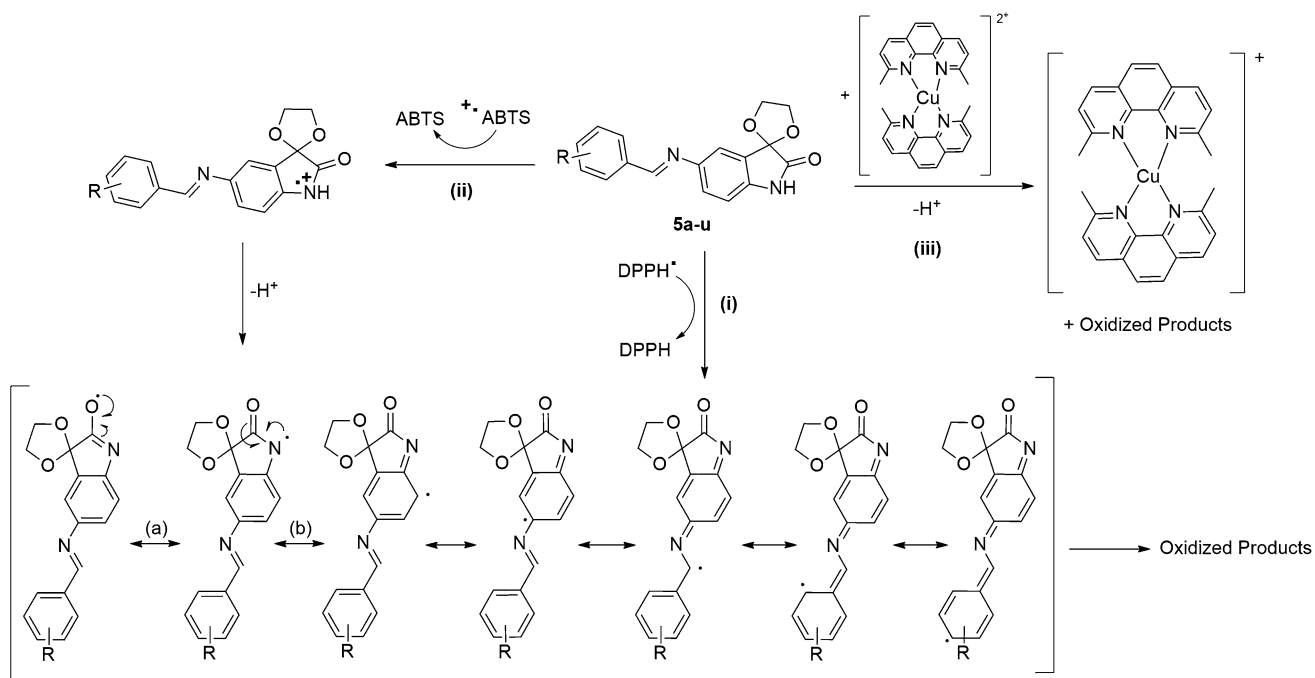


Fig. 3 The proposed mechanism of the synthesized compounds for antioxidant assays; (i) DPPH, (ii) ABTS, (iii) CUPRAC

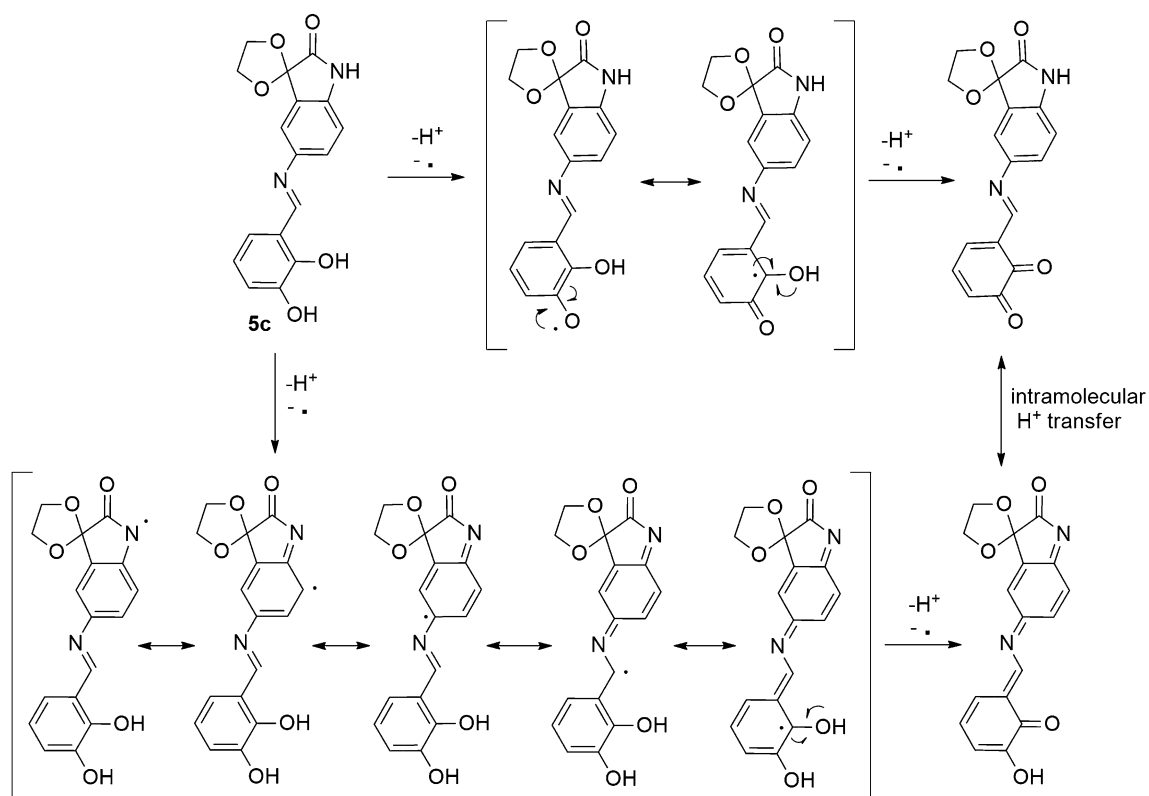


Fig. 4 The formation of quinone by oxidizing **5c**

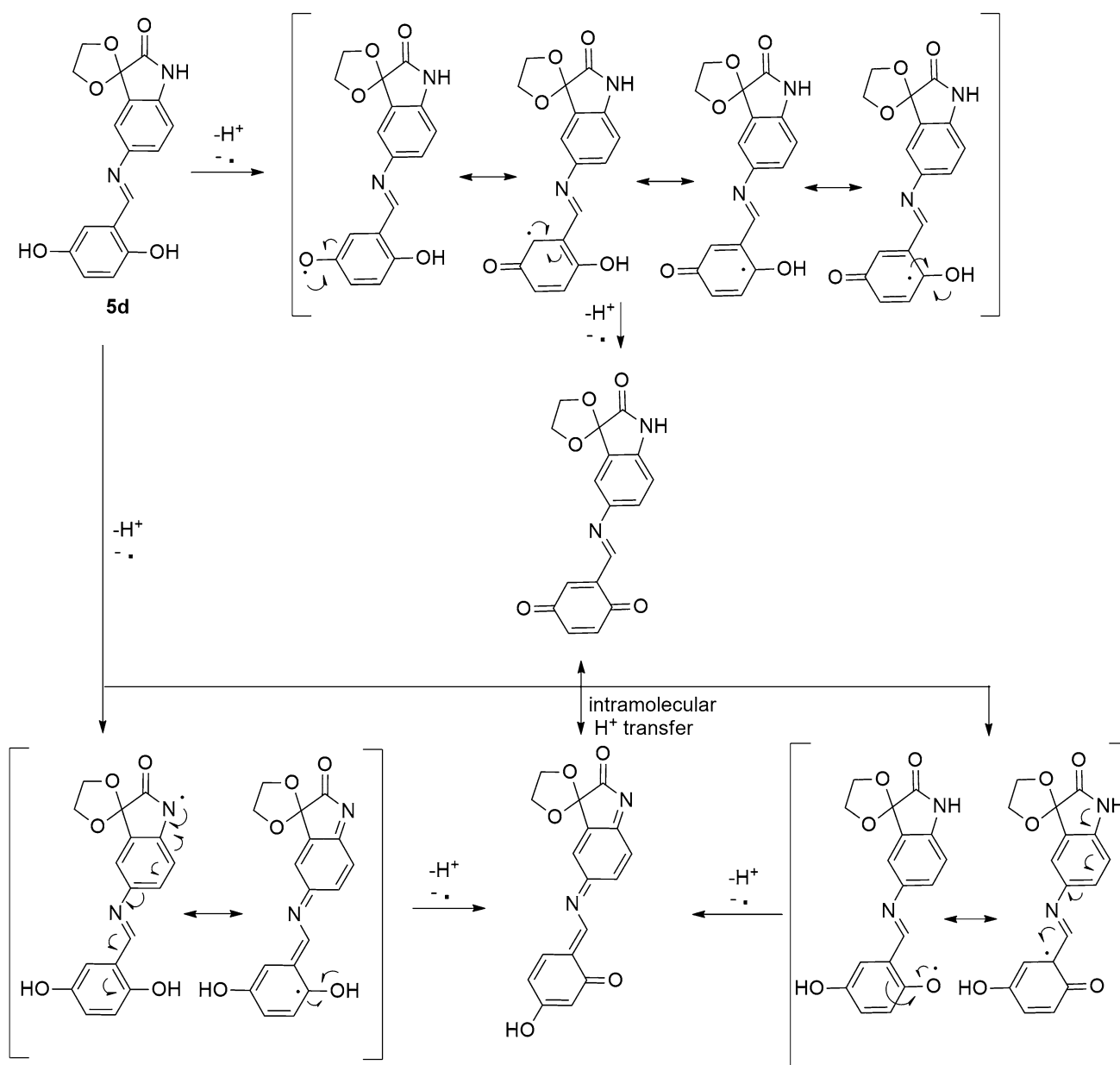


Fig. 5 The formation of quinone by oxidizing **5d**

so much less or the similar cupric reducing antioxidant capacity than quercetin (Table 1).

The synthesized compounds include the indole ring, phenyl ring and the imine moiety as a linker between these rings. The presence of this imine group allows for conjugation between two aromatic rings and thus increases the resonance stabilization over the whole molecule. The high electron conjugation makes the formed radical more stable. Consequently, it considers that this feature enhances the ability of the synthesized compounds for acting as a potent antioxidant [36, 37]. The predicted mechanism of the synthesized compounds to act as a scavenger can propose as

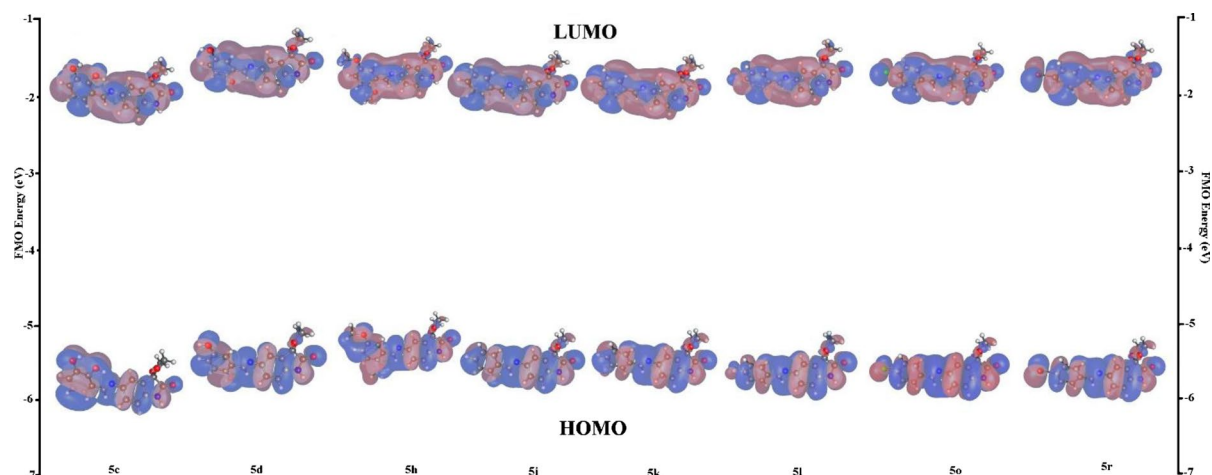
shown in Fig. 3. According to this proposed mechanism, the possible products of the best antioxidant compounds (**5c** and **5d**) in this study are given in Figs. 4 and 5, respectively. These two compounds have phenolic moiety, so it is possible they can be converted to the corresponding quinones after the antioxidant assays. It is known that quinones are used as drugs to treat human cancer. Most of the quinones having antitumor activity can expose reversible enzymatic reduction and oxidation. The antitumor activity of quinones is related to DNA damage caused by alkylating species or oxygen radicals [38]. Therefore, this formation of quinones may be advantageous to treat some disease.

Structure–activity relationships (SAR)

Generally, the synthesized compounds had higher ABTS⁺ activity than DPPH and CUPRAC activities. Moreover, the compounds (**5c** and **5d**), containing two hydroxyl groups, exhibited the strongest antioxidant activities for all assays.

The following structure–activity relationship (SAR) observations can also be drawn from data of Table 1:

1. The presence of OH group on the phenyl ring increased the antioxidant activities (comparing **5a** (R = H, IC₅₀ = 171.74 μM and 18.45 μM for DPPH and ABTS⁺, respectively; A_{0.50} = 75.87 μM for CUPRAC) with **5b** (R = 3-OH, IC₅₀ = 94.81 μM and 1.93 μM for DPPH and ABTS⁺, respectively; A_{0.50} = 18.76 μM for CUPRAC)). In addition, the binding of the second –OH group to the phenyl ring caused a significant increase for all the antioxidant activities (comparing **5b** (R = 3-OH) with **5c** (R = 2,3-di-OH, IC₅₀ = 4.49 μM and 0.39 μM for DPPH and ABTS⁺, respectively; A_{0.50} = 0.42 μM for CUPRAC) and **5d** (R = 2,5-di-OH, IC₅₀ = 18.65 μM and 0.86 μM for DPPH and ABTS⁺, respectively; A_{0.50} = 1.35 μM for CUPRAC)). On the other hand, the presence of the third –OH group on the phenyl ring decreased the antioxidant activities (comparing **5c** (R = 2,3-di-OH) and **5d** (R = 2,5-di-OH) with **5e** (R = 2,4,6-tri-OH, IC₅₀ = 64.03 μM and 1.57 μM for DPPH and ABTS⁺, respectively; A_{0.50} = 12.99 μM for CUPRAC)); however, **5e** still had higher antioxidant activities than **5a** (R = H) and **5b** (R = 3-OH).
2. The compounds (**5b** (R = 3-OH), **5c** (R = 2,3-di-OH) and **5d** (R = 2,5-di-OH)), containing one or two hydroxyl groups, exhibited better antioxidant activities than the compounds (**5f** (R = 4-OCH₃, IC₅₀ = 145.00 μM and 6.83 μM for DPPH and ABTS⁺, respectively; A_{0.50} = 28.74 μM for CUPRAC), **5g** (R = 3,4-di-OCH₃, IC₅₀ = 130.00 μM and 1.45 μM for DPPH and ABTS⁺, respectively; A_{0.50} = 28.06 μM for CUPRAC) and **5h** (R = 2,5-di-OCH₃, IC₅₀ = 81.78 μM and 0.95 μM for DPPH and ABTS⁺, respectively; A_{0.50} = 17.59 μM for CUPRAC)), containing one or two methoxy groups. On the other hand, the presence of the second –OCH₃ group on the phenyl ring decreased the antioxidant activities (comparing **5f** (R = 4-OCH₃) with **5c** (R = 2,3-di-OH) and **5d** (R = 2,5-di-OH)).
3. The exchanging methoxy group at *para*-position of phenyl ring with dimethylamine group increased the antioxidant activities (comparing **5f** (R = 4-OCH₃, IC₅₀ = 145.00 μM and 6.83 μM for DPPH and ABTS⁺, respectively; A_{0.50} = 28.74 μM for CUPRAC) with **5i** (R = 4-N(CH₃)₂, IC₅₀ = 112.33 μM and 1.56 μM for DPPH and ABTS⁺, respectively; A_{0.50} = 15.38 μM for CUPRAC)).
4. Moving the halogen atoms (F, Cl or Br) on the phenyl ring from *ortho*-position to *meta*- and *para*-positions led to an increase in ABTS⁺ and CUPRAC activities (comparing **5j** (R = 2-F, IC₅₀ = 1.25 μM for ABTS⁺ and A_{0.50} = 29.38 μM for CUPRAC) with **5k** (R = 3-F, IC₅₀ = 1.06 μM for ABTS⁺ and A_{0.50} = 24.76 μM for CUPRAC) and **5l** (R = 4-F, IC₅₀ = 0.98 μM for ABTS⁺ and A_{0.50} = 16.99 μM for CUPRAC)); comparing **5m** (R = 2-Cl, IC₅₀ = 2.43 μM for ABTS⁺ and A_{0.50} = 26.31 μM for CUPRAC) with **5n** (R = 3-Cl, IC₅₀ = 1.48 μM for ABTS⁺ and A_{0.50} = 18.13 μM for CUPRAC) and **5o** (R = 4-Cl, IC₅₀ = 1.28 μM for ABTS⁺ and A_{0.50} = 16.67 μM for CUPRAC)); comparing **5p** (R = 2-Br, IC₅₀ = 1.85 μM for ABTS⁺ and A_{0.50} = 20.92 μM for CUPRAC) with **5q** (R = 3-Br, IC₅₀ = 1.45 μM for ABTS⁺ and A_{0.50} = 16.90 μM for CUPRAC) and **5r** (R = 4-Br, IC₅₀ = 1.24 μM for ABTS⁺ and A_{0.50} = 16.15 μM for CUPRAC)). On the other hand, the compounds (**5k** (R = 3-F, IC₅₀ = 137.75 μM for DPPH), **5n** (R = 3-Cl, IC₅₀ = 178.91 μM for DPPH) and **5q** (R = 3-Br, IC₅₀ = 204.90 μM for DPPH)), containing halogens at the *meta*-position of the phenyl ring, showed lower DPPH activity than the compounds (**5j** (R = 2-F, IC₅₀ = 125.40 μM for DPPH), **5m** (R = 2-Cl, IC₅₀ = 129.40 μM for DPPH) and **5p** (R = 2-Br, IC₅₀ = 143.90 μM for DPPH)), containing halogens at the *ortho*-position. In addition, the compounds (**5l** (R = 4-F, IC₅₀ = 90.15 μM for DPPH), **5o** (R = 4-Cl, IC₅₀ = 110.95 μM for DPPH) and **5r** (R = 4-Br, IC₅₀ = 127.16 μM for DPPH)), containing halogens at the *para*-position of the phenyl ring, exhibited the highest DPPH activity among the halogen series.
5. The DPPH and CUPRAC activities seem to be strongly dependent on the size and polarizability of the halogen substituent at the *ortho*-, *meta*- and *para*-positions of the phenyl ring. The DPPH activity of the compounds containing halogens decreased with the growing size of the halogens, whereas CUPRAC activity of them increased (for size and polarizability, Br > Cl > F; for DPPH activity, **5j** (R = 2-F, IC₅₀ = 125.40 μM) > **5m** (R = 2-Cl, IC₅₀ = 129.40 μM) > **5p** (R = 2-Br, IC₅₀ = 143.90 μM); **5k** (R = 3-F, IC₅₀ = 137.75 μM) > **5n** (R = 3-Cl, IC₅₀ = 178.91 μM) > **5q** (R = 3-Br, IC₅₀ = 204.90 μM); **5l** (R = 4-F, IC₅₀ = 90.15 μM) > **5o** (R = 4-Cl, IC₅₀ = 110.95 μM) > **5r** (R = 4-Br, IC₅₀ = 127.16 μM); for CUPRAC activity, **5p** (R = 2-Br, A_{0.50} = 20.92 μM) > **5m** (R = 2-Cl, A_{0.50} = 26.31 μM) > **5j** (R = 2-F, A_{0.50} = 29.38 μM); **5q** (R = 3-Br, A_{0.50} = 16.90 μM) > **5n** (R = 3-Cl, A_{0.50} = 18.13 μM) > **5k** (R = 3-F, A_{0.50} = 24.76 μM); **5r** (R = 4-Br, A_{0.50} = 16.15 μM) > **5o** (R = 4-Cl, A_{0.50} = 16.67 μM) > **5l** (R = 4-F, A_{0.50} = 16.99 μM)). This relation was not observed for the ABTS⁺ activity.

Table 2 FMO energies of the selected compounds

| Comp. | R | E_{HOMO} (eV) | E_{LUMO} (eV) | ΔE (eV) | A (eV) | η (eV) | S (eV) ⁻¹ | χ (eV) | E_{tot} (au) |
|-----------|-------------------------|------------------------|------------------------|-----------------|----------|-------------|------------------------|-------------|-----------------------|
| 5c | 2,3-di-OH | -5.905 | -2.068 | 3.837 | 2.068 | 1.919 | 0.521 | 3.987 | -1090.91 |
| 5d | 2,5-di-OH | -5.660 | -1.823 | 3.837 | 1.823 | 1.919 | 0.521 | 3.742 | -1142.13 |
| 5h | 2,5-di-OCH ₃ | -5.605 | -1.769 | 3.836 | 1.769 | 1.918 | 0.521 | 3.687 | -1220.75 |
| 5j | 2-F | -5.905 | -2.041 | 3.864 | 2.041 | 1.932 | 0.518 | 3.973 | -1142.15 |
| 5k | 3-F | -5.986 | -2.068 | 3.918 | 2.068 | 1.959 | 0.510 | 4.027 | -1090.91 |
| 5l | 4-F | -5.959 | -2.122 | 3.837 | 2.122 | 1.919 | 0.521 | 4.041 | -1090.91 |
| 5o | 4-Cl | -5.959 | -2.095 | 3.864 | 2.095 | 1.932 | 0.518 | 4.027 | -1451.27 |
| 5r | 4-Br | -5.905 | -1.932 | 3.973 | 1.932 | 1.987 | 0.503 | 3.919 | -3565.19 |

A electron affinity, η chemical hardness, χ electronegativity, S chemical softness, E total energy

6. Moving the nitro groups on the phenyl ring from *ortho*-position to *meta*- and *para*-positions led to an increase in DPPH and ABTS⁺ activities (comparing **5s** (R=2-NO₂, IC₅₀=162.91 μM and 19.20 μM for DPPH and ABTS⁺, respectively) with **5t** (R=3-NO₂, IC₅₀=126.62 μM and 1.56 μM for DPPH and ABTS⁺, respectively) and **5u** (R=4-NO₂, IC₅₀=118.86 μM and 1.38 μM for DPPH and ABTS⁺, respectively)); however, it led to a decrease in the CUPRAC activity (comparing **5s** (R=2-NO₂, A_{0.50}=15.12 μM for CUPRAC) with **5t** (R=3-NO₂, A_{0.50}=19.23 μM for CUPRAC) and **5u** (R=4-NO₂, A_{0.50}=26.03 μM for CUPRAC)).

In addition, some electronic parameters (the highest occupied molecular orbital and the lowest unoccupied molecular orbital (HOMO–LUMO) energy levels, electronegativity, chemical hardness and softness, total energy and dipole moments) of the selected compounds were calculated to support and enrich the SAR of obtained experimental results (Table 2). For quantum chemical calculations, **5c** was selected because of the best inhibitor, **5d** and **5h** were selected to compare the effects of -OH and

-OCH₃ at the same position, **5j**, **5k** and **5l** were chosen due to comparing the effects of the substituent position, and **5l**, **5o** and **5r** were selected to investigate halogen series at the same position.

It is well known that the molecular chemical stability, chemical reactivity and spectroscopic properties of the compounds are connected with the relationship between energy gap and the frontier molecular orbitals (FMOs). Generally, highest occupied molecular orbital (HOMO) and lowest unoccupied molecular orbital (LUMO) energies are related to electron affinity. These FMOs are associated with the molecule's reactivity. HOMO energy is closely related to susceptibility to electrophilic attack, while LUMO energy is closely related to susceptibility to nucleophilic attack [39, 40].

Rising the LUMO energies decreased the antioxidant activities (comparing **5c** ($E_{\text{LUMO}} = -2.068$ eV) with **5d** ($E_{\text{LUMO}} = -1.823$ eV) and **5h** ($E_{\text{LUMO}} = -1.769$ eV), **5c** > **5d** > **5h** for each antioxidant activity; comparing **5j** ($E_{\text{LUMO}} = -2.041$ eV) with **5k** ($E_{\text{LUMO}} = -2.068$ eV) and **5l** ($E_{\text{LUMO}} = -2.122$ eV), **5l** > **5k** > **5j** for ABTS and CUPRAC activity, **5l** > **5j** ~ **5k** for DPPH activity; comparing **5l**

($E_{\text{LUMO}} = -2.122$ eV) with **5o** ($E_{\text{LUMO}} = -2.095$ eV) and **5r** ($E_{\text{LUMO}} = -1.932$ eV), **5l** > **5o** > **5r** for DPPH activity, **5l** > **5o** ~ **5r** for ABTS activity; **5l** ~ **5o** ~ **5r** for CUPRAC activity). It is known that low LUMO energy increases the acceptor properties of the molecules, and they can get electrons easily.

The electronegativity of the molecules showed a linear relationship with the increasing antioxidant activity (comparing **5c** ($\chi = 3.987$ eV) with **5d** ($\chi = 3.742$ eV) and **5h** ($\chi = 3.687$ eV), **5c** > **5d** > **5h** for each antioxidant activity; comparing **5j** ($\chi = 3.973$ eV) with **5k** ($\chi = 4.027$ eV) and **5l** ($\chi = 4.041$ eV), **5l** > **5k** > **5j** for ABTS and CUPRAC activity, **5l** > **5j** ~ **5k** for DPPH activity; comparing **5l** ($\chi = 4.041$ eV) with **5o** ($\chi = 4.027$ eV) and **5r** ($\chi = 3.919$ eV), **5l** > **5o** > **5r** for DPPH activity, **5l** > **5o** ~ **5r** for ABTS activity; **5l** ~ **5o** ~ **5r** for CUPRAC activity). This relationship can be explained that the high electronegativity increases the electron affinity of the molecule and so its antioxidant activity is enhanced. Also, the high electronegativity of molecule can give stability to occurring radical.

It was seen that **5c**, **5d** and **5h** have same chemical hardness (η) and softness (S). On the other hand, increasing chemical softness and conversely decreasing chemical hardness enhanced the antioxidant activity comparing **5j** ($\eta = 1.932$ eV, $S = 0.518$ (eV)⁻¹) with **5k** ($\eta = 1.959$ eV, $S = 0.510$ (eV)⁻¹) and **5l** ($\eta = 1.919$ eV, $S = 0.521$ (eV)⁻¹), **5l** > **5j** > **5k** for DPPH activity, **5l** > **5k** > **5j** for ABTS and CUPRAC activity; comparing **5l** ($\eta = 1.919$ eV, $S = 0.521$ (eV)⁻¹) with **5o** ($\eta = 1.932$ eV, $S = 0.518$ (eV)⁻¹) and **5r** ($\eta = 1.987$ eV, $S = 0.503$ (eV)⁻¹), **5l** > **5o** > **5r** for DPPH activity, **5l** > **5o** ~ **5r** for ABTS activity; **5l** ~ **5o** ~ **5r** for CUPRAC activity). According to “hard and soft (Lewis) acids and bases” (HSAB) theory, soft acids react faster and form stronger bonds with soft bases, whereas hard acids react faster and form stronger bonds with hard bases [41]. Radicals are soft both as an acceptor or donor [42]. Therefore, raising softness of the molecule can increase its antioxidant activity as expected.

These quantum chemical calculations support structure–activity relationship of the compounds including similar group; however, considering all molecules, there are some contradictions. It is clear that the antioxidant activities of the compounds not only depend on their LUMO energies, electronegativity or chemical hardness/softness, but also on resonance stability of the formed radical significant effects on antioxidant activity.

Conclusion

In conclusion, a series of 21 novel Schiff base-substituted spiro-isatin derivatives (**5a–u**) was synthesized and their antioxidant activities were evaluated. In addition,

structure–activity relationship was presented and also it was supported with quantum chemical calculations. All the synthesized compounds exhibited higher ABTS cation radical scavenging ability than DPPH and CUPRAC activities. **5c**, containing two hydroxyl groups on the phenyl ring, had the most potent antioxidant activity according to three different antioxidant activity methods. The SAR study revealed that the antioxidant activity of the synthesized compounds could also be influenced by the type and position of substituent on the phenyl ring. In particular, the presence of the hydroxyl groups and the position and size of the halogens on the phenyl ring were seen to play a key role for antioxidant activity. The quantum chemical calculations showed that the LUMO energies, electronegativity and chemical softness of the molecules were effective on their antioxidant activities.

Experimental

General methods

Melting points were measured on a Barnstead Electrothermal 9200. IR spectra were measured on a Shimadzu Prestige-21 (200 VCE) spectrometer. ¹H and ¹³C NMR spectra were measured on a Varian Infinity Plus spectrometer at 300 and at 75 Hz, respectively. ¹H and ¹³C chemical shifts are referenced to the internal deuterated solvent. Mass spectra were obtained using MICROMASS Quattro LC–MS–MS spectrometer. The elemental analyses were performed with a Leco CHNS-932 instrument. Spectrophotometric analyses were performed by a BioTek Power Wave XS (BioTek, USA). The chemicals and solvents were purchased from Fluka Chemie, Merck, Alfa Easer and Sigma-Aldrich.

Synthesis procedures and spectral data

5-Nitroindoline-2,3-dione (2) 3 mmol of KNO₃ and H₂SO₄ was stirred in an ice bath. 3 mmol of isatin was slowly added to this mixture. The mixture was stirred for 2 h at room temperature. Finally, it was poured into ice, the precipitate was filtered off and dried under vacuum.

Yellow powder, 96% yield, ¹H NMR (DMSO-*d*₆, 300 MHz) δ /ppm: 7.07 (1H, d, $J = 8.7$ Hz), 8.18 (1H, d, $J = 2.0$ Hz), 8.41–8.43 (1H, dd, $J = 2.0, 8.5$ Hz), 11.66 (1H, s, NH). ¹³C NMR (DMSO-*d*₆, 75 MHz) δ /ppm: 113.2, 118.8, 120.3, 133.8, 143.2, 155.8, 160.6, 183.0.

5'-Nitrospiro[[1,3] dioxolane-2,3'-indolin]-2'-one (3) 15 mmol of 5-nitroindoline-2,3-dione (**2**), 60 mmol of ethylene glycol and 3 mmol of p-toluene sulphonic acid (PTSA) in benzene were stirred in a Dean–Stark apparatus at reflux temperature for 24 h. The mixture was cooled and

evaporated in vacuum. The residue was extracted with ethyl acetate (3 × 50 mL), and the organic phase was washed with aqueous NaHCO₃. It was dried with MgSO₄ and evaporated in vacuum.

Yellowish powder, 83% yield, ¹H NMR (CDCl₃+DMSO-d₆, 300 MHz) δ/ppm: 4.34–4.42 (2H, m), 4.50–4.58 (2H, m), 6.96 (1H, d, *J* = 8.8 Hz), 8.19 (1H, d, *J* = 2.3 Hz), 8.22–8.25 (1H, dd, *J* = 2.3, 8.8 Hz), 10.60 (1H, s, NH); ¹³C NMR (CDCl₃+DMSO-d₆, 75 MHz) δ/ppm: 66.2, 101.4, 111.0, 121.3, 125.6, 128.5, 143.4, 149.4, 175.5.

5'-Aminospiro[[1,3] dioxolane-2,3'-indolin]-2'-one

(4) 7.5 mmol of 5'-nitrospiro[[1,3] dioxolane-2,3'-indolin]-2'-one (**3**) was dissolved in anhydrous ethanol. 37 mmol of cyclohexene and 3.975 g of 10% Pd–C were added to this solution. The mixture was refluxed for 2 h. It was cooled and filtered to separate solid Pd–C. The solution was evaporated, and the product was recrystallized with ethanol.

Brown powder, 87% yield, IR: 3398, 3374, 3319, 3161, 2902, 2812, 1741, 1716, 1697, 1622, 1490, 1477, 1211, 1080, 993, 742, 640 cm⁻¹; ¹H NMR (DMSO-d₆, 300 MHz) δ/ppm: 4.16–4.24 (2H, m), 4.27–4.35 (2H, m), 4.85 (2H, s, NH₂), 6.52 (2H, d, *J* = 1.5 Hz), 6.59 (1H, d, *J* = 1.5 Hz), 9.99 (1H, s, NH); ¹³C NMR (DMSO-d₆, 75 MHz) δ/ppm: 66.0, 102.9, 111.5, 112.2, 116.7, 125.8, 132.7, 145.0, 174.9; LC–MS (*m/z*): 207.13 [MH⁺].

Synthesis of 5'-(benzylideneamino)spiro[[1,3] dioxolane-2,3'-indolin]-2'-one derivatives (5a–u)

10 mmol of 5'-aminospiro[[1,3] dioxolane-2,3'-indolin]-2'-one (**4**), 12 mmol of various aldehyde derivatives and 0.05 mmol of Et₃N in EtOH were refluxed for 8 h. The mixture was cooled and evaporated in vacuum. The crude product was washed with chloroform and dried in vacuum.

(E)-5'-(benzylideneamino)spiro[[1,3] dioxolane-2,3'-indolin]-2'-one (5a)

Dark brown powder, 75% yield, mp. 204.3–205.8 °C; IR: 3232, 2993, 2907, 1728, 1697, 1623, 1479, 1286, 1216, 1066, 834, 753, 691, 612 cm⁻¹; ¹H NMR (DMSO-d₆, 300 MHz) δ/ppm: 4.25–4.29 (2H, m), 4.30–4.35 (2H, m), 6.89 (1H, d, *J* = 8.2 Hz), 7.31–7.34 (1H, dd, *J*₁ = 2.0 Hz; *J*₂ = 8.2 Hz), 7.39 (1H, s), 7.51–7.53 (3H, m), 7.92 (2H, t, *J* = 3.8 Hz), 8.69 (1H, s), 10.55 (1H, s, NH); ¹³C NMR (DMSO-d₆, 75 MHz) δ/ppm: 66.3, 102.4, 111.7, 118.0, 126.3, 126.4, 129.2, 129.5, 131.9, 136.9, 141.7, 146.8, 159.8, 175.2; LC–MS (*m/z*): 295, 1135 [MH⁺]. Anal. Calcd. for C₁₇H₁₄N₂O₃: C, 69.38; H, 4.79; N, 9.52; found: C, 69.34; H, 4.76; N, 9.57.

(E)-5'-((3-hydroxybenzylidene)amino)spiro[[1,3] dioxolane-2,3'-indolin]-2'-one (5b)

Brown powder, 83% yield, mp. 248.5–249.6 °C; IR: 3395, 3175, 2970, 2904, 1736, 1628, 1578, 1489, 1221, 1186, 992, 777,

683 cm⁻¹; ¹H NMR (DMSO-d₆, 300 MHz) δ/ppm: 4.25–4.29 (2H, m), 4.33–4.38 (2H, m), 6.88 (2H, td, *J*₁ = 2.4 Hz, *J*₂ = 7.3 Hz), 7.27–7.35 (5H, m), 8.57 (1H, s), 9.68 (1H, s, OH), 10.51 (1H, s, NH); ¹³C NMR (DMSO-d₆, 75 MHz) δ/ppm: 66.3, 102.4, 111.7, 111.8, 118.0, 111.3, 120.9, 126.2, 126.4, 130.5, 138.2, 141.7, 146.8, 158.3, 159.8, 175.2; LC–MS (*m/z*): 311.2070 [MH⁺]. Anal. Calcd. for C₁₇H₁₄N₂O₄: C, 65.80; H, 4.55; N, 9.03; found: C, 65.85; H, 4.51; N, 9.07.

(E)-5'-((2,3-dihydroxybenzylidene)amino)spiro[[1,3] dioxolane-2,3'-indolin]-2'-one (5c)

Dark brown powder, 85.8% yield, mp. 265.5–266.9 °C; IR: 3440, 3092, 2981, 2905, 1727, 1627, 1467, 1213, 1066, 1028, 938, 729 cm⁻¹; ¹H NMR (DMSO-d₆, 300 MHz) δ/ppm: 4.28–4.33 (2H, m), 4.36–4.40 (2H, m), 6.78 (1H, t, *J* = 7.6 Hz), 6.92–6.95 (2H, m), 7.07–7.09 (1H, dd, *J*₁ = 1.2 Hz, *J*₂ = 7.8 Hz), 7.41–7.44 (1H, dd, *J*₁ = 2.0 Hz, *J*₂ = 8.2 Hz), 7.55 (1H, d, *J* = 2.0 Hz), 8.95 (1H, s), 9.18 (1H, s, OH), 10.61 (1H, s, NH), 13.17 (1H, s, OH); ¹³C NMR (DMSO-d₆, 75 MHz) δ/ppm: 66.3, 102.3, 111.9, 118.1, 119.0, 119.4, 120.1, 123.4, 126.5, 126.7, 142.3, 143.5, 146.2, 149.7, 162.9, 175.2; LC–MS (*m/z*): 349.1845 [MNa⁺]. Anal. Calcd. for C₁₇H₁₄N₂O₅: C, 62.57; H, 4.32; N, 8.59; found: C, 62.54; H, 4.36; N, 8.55.

(E)-5'-((2,5-dihydroxybenzylidene)amino)spiro[[1,3] dioxolane-2,3'-indolin]-2'-one (5d)

Brown powder, 87.2% yield, mp. 279.9–281.4 °C; IR: 3394, 3151, 2968, 2896, 1739, 1626, 1486, 1276, 1220, 1188, 993, 757 cm⁻¹; ¹H NMR (DMSO-d₆, 300 MHz) δ/ppm: 4.30–4.32 (2H, m), 4.35–4.40 (2H, m), 6.77–6.87 (2H, m), 6.90 (1H, d, *J* = 8.2 Hz), 7.01 (1H, d, *J* = 2.6 Hz), 7.38–7.41 (1H, dd, *J*₁ = 2.3 Hz, *J*₂ = 8.2 Hz), 7.52 (1H, d, *J* = 1.7 Hz), 8.88 (1H, s), 9.10 (1H, s, OH), 10.59 (1H, s, NH), 12.30 (1H, s, OH); ¹³C NMR (DMSO-d₆, 75 MHz) δ/ppm: 66.3, 102.3, 111.9, 117.6, 117.8, 118.2, 120.0, 121.5, 126.5, 126.6, 142.2, 143.9, 150.3, 153.7, 162.2, 175.2; LC–MS (*m/z*): 327.2204 [MH⁺]. Anal. Calcd. for C₁₇H₁₄N₂O₅: C, 62.57; H, 4.32; N, 8.59; found: C, 62.53; H, 4.35; N, 8.56.

(E)-5'-((2,4,6-trihydroxybenzylidene)amino)spiro[[1,3] dioxolane-2,3'-indolin]-2'-one (5e)

Dark brown powder, 95% yield, mp. 257.3–257.6 °C; IR: 3174, 2970, 1726, 1619, 1579, 1492, 1281, 1197, 1170, 1135, 1072, 941, 814 cm⁻¹; ¹H NMR (DMSO-d₆, 300 MHz) δ/ppm: 4.27–4.31 (2H, m), 4.33–4.37 (2H, m), 5.82 (2H, s), 6.86 (1H, d, *J* = 8.5 Hz), 7.27–7.25 (1H, dd, *J*₁ = 2.0 Hz, *J*₂ = 8.5 Hz), 7.35 (1H, d, *J* = 2.0 Hz), 8.90 (1H, s), 10.10 (1H, br, OH), 10.55 (1H, s, NH); ¹³C NMR (DMSO-d₆, 75 MHz) δ/ppm: 66.3, 94.8, 102.1, 102.3, 111.9, 117.9, 125.2, 126.7, 141.3, 144.2, 157.1, 164.2, 164.8, 175.2; LC–MS (*m/z*): 381.3689 [MK⁺]. Anal. Calcd. for C₁₇H₁₄N₂O₆: C, 59.65; H, 4.12; N, 8.18; found: C, 59.68; H, 4.10; N, 8.14.

(E)-5'-((4-methoxybenzylidene)amino)spiro[[1,3]dioxolane-2,3'-indolin]-2'-one (5f) Brown powder, 79% yield, mp. 218.8–220.2 °C; IR: 3140, 3042, 2894, 2839, 1721, 1630, 1606, 1510, 1474, 1246, 1162, 1070, 1027, 995, 827, 607 cm⁻¹; ¹H NMR (DMSO-d₆, 300 MHz) δ/ppm: 3.81 (3H, s), 4.27–4.34 (4H, m), 6.85 (1H, d, *J* = 8.2 Hz), 7.05 (2H, d, *J* = 8.5 Hz), 7.26 (1H, d, *J* = 8.2 Hz), 7.32 (1H, s), 7.86 (2H, d, *J* = 8.5 Hz), 8.57 (1H, s), 10.50 (1H, s, NH); ¹³C NMR (DMSO-d₆, 75 MHz) δ/ppm: 56.1, 66.2, 102.4, 111.7, 114.9, 117.9, 126.0, 126.4, 129.7, 130.9, 141.2, 147.1, 159.0, 162.4, 175.2; LC–MS (*m/z*): 325.1615[MH⁺]. Anal. Calcd. for C₁₈H₁₆N₂O₄: C, 66.66; H, 4.97; N, 8.64; found: C, 66.60; H, 4.95; N, 8.68.

(E)-5'-((3,4-dimethoxybenzylidene)amino)spiro[[1,3]dioxolane-2,3'-indolin]-2'-one (5g) Orange powder, 84% yield, mp. 134.8–136.9 °C; IR: 3242, 2902, 2835, 1729, 1631, 1581, 1512, 1263, 1193, 1142, 1068, 1022, 943, 752, 629 cm⁻¹; ¹H NMR (DMSO-d₆, 300 MHz) δ/ppm: 3.84 (6H, s), 4.29–4.31 (2H, m), 4.34–4.36 (2H, m), 6.87 (1H, d, *J* = 8.2 Hz), 7.09 (1H, d, *J* = 8.5 Hz), 7.27–7.29 (1H, dd, *J*₁ = 1.8 Hz, *J*₂ = 8.2 Hz), 7.35 (1H, d, *J* = 1.8 Hz), 7.45 (1H, d, *J* = 8.2 Hz), 7.54 (1H, s), 8.57 (1H, s), 10.52 (1H, s, NH); ¹³C NMR (DMSO-d₆, 75 MHz) δ/ppm: 56.0, 56.3, 66.3, 102.4, 109.9, 111.7, 111.9, 117.9, 124.5, 126.0, 126.4, 129.8, 141.2, 147.1, 149.6, 152.3, 159.3, 175.2; LC–MS (*m/z*): 355.2162 [MH⁺]. Anal. Calcd. for C₁₉H₁₈N₂O₅: C, 64.40; H, 5.12; N, 7.91; found: C, 64.44; H, 5.15; N, 7.87.

(E)-5'-((2,5-dimethoxybenzylidene)amino)spiro[[1,3]dioxolane-2,3'-indolin]-2'-one (5h) Brown powder, 71% yield, mp. 183.8–186.1 °C; IR: 3139, 3103, 2954, 2905, 2834, 1724, 1624, 1493, 1275, 1213, 1022, 946, 787, 707, 634 cm⁻¹; ¹H NMR (DMSO-d₆, 300 MHz) δ/ppm: 3.75 (3H, s), 3.83 (3H, s), 4.27–4.29 (2H, m), 4.31–4.34 (2H, m), 6.85 (1H, d, *J* = 7.9 Hz), 7.08 (2H, d, *J* = 2.7 Hz), 7.25 (1H, d, *J* = 8.2 Hz), 7.28 (1H, s), 7.50 (1H, s), 8.80 (1H, s), 10.51 (1H, s, NH); ¹³C NMR (DMSO-d₆, 75 MHz) δ/ppm: 56.1, 56.9, 66.3, 102.4, 110.7, 111.8, 114.2, 118.3, 119.9, 125.0, 125.7, 126.5, 141.6, 147.4, 153.8, 154.4, 159.5, 175.2; LC–MS (*m/z*): 377.2217[MNa⁺]. Anal. Calcd. for C₁₉H₁₈N₂O₅: C, 64.40; H, 5.12; N, 7.91; found: C, 64.45; H, 5.16; N, 7.86.

(E)-5'-((4-(dimethylamino)benzylidene)amino)spiro[[1,3]dioxolane-2,3'-indolin]-2'-one (5i) Orange powder, 94.4% yield, mp. 252.6–254.4 °C; IR: 3220, 2899, 1737, 1698, 1589, 1475, 1364, 1198, 1166, 1065, 940, 816 cm⁻¹; ¹H NMR (DMSO-d₆, 300 MHz) δ/ppm: 3.00 (3H, s), 3.04 (3H, s), 4.28–4.31 (2H, m), 4.33–4.36 (2H, m), 6.77 (2H, d, *J* = 8.8 Hz), 6.83 (1H, d, *J* = 8.2 Hz), 7.20–7.22 (1H, dd, *J*₁ = 2.1 Hz, *J*₂ = 8.2 Hz), 7.28 (1H, d, *J* = 2.0 Hz), 7.73 (2H, d, *J* = 8.8 Hz), 8.45 (1H, s), 10.46 (1H, s, NH); ¹³C

NMR (DMSO-d₆, 75 MHz) δ/ppm: 40.3, 66.2, 102.5, 111.6, 112.1, 117.8, 124.5, 125.6, 126.4, 130.8, 140.6, 147.8, 152.9, 159.3, 175.2; LC–MS (*m/z*): 360.2523[MNa⁺]. Anal. Calcd. for C₁₉H₁₉N₃O₃: C, 67.64; H, 5.68; N, 12.46; found: C, 67.60; H, 5.70; N, 12.43.

(E)-5'-((2-fluorobenzylidene)amino)spiro[[1,3]dioxolane-2,3'-indolin]-2'-one (5j) Brown powder, 62% yield, mp. 244.9–247.4 °C; IR: 3104, 3038, 2896, 1729, 1627, 1474, 1452, 1278, 1213, 1074, 1000, 834, 763, 634 cm⁻¹; ¹H NMR (DMSO-d₆, 300 MHz) δ/ppm: 4.26–4.30 (2H, m), 4.32–4.37 (2H, m), 6.87 (1H, d, *J* = 8.2 Hz), 7.30–7.36 (3H, m), 7.41 (1H, d, *J* = 2.0 Hz), 7.53–7.60 (1H, qd, *J*₁ = 1.8 Hz, *J*₂ = 5.5 Hz), 8.04–8.09 (1H, td, *J*₁ = 1.6 Hz, *J*₂ = 7.6 Hz), 8.79 (1H, s), 10.55 (1H, s, NH); ¹³C NMR (DMSO-d₆, 75 MHz) δ/ppm: 66.3, 102.3, 111.7, 116.7, 116.9, 118.3, 124.3, 125.6, 126.3, 128.3, 134.1, 142.1, 146.6, 152.3, 164.4, 175.2; LC–MS (*m/z*): 335.2516[MNa⁺]. Anal. Calcd. for C₁₇H₁₃FN₂O₃: C, 65.38; H, 4.20; N, 8.97; found: C, 65.35; H, 4.22; N, 8.96.

(E)-5'-((3-fluorobenzylidene)amino)spiro[[1,3]dioxolane-2,3'-indolin]-2'-one (5k) Brown powder, 62% yield, mp. 227.5–229.1 °C; IR: 3232, 2974, 2907, 1728, 1697, 1625, 1482, 1450, 1215, 1066, 993, 941, 751, 685, 617 cm⁻¹; ¹H NMR (DMSO-d₆, 300 MHz) δ/ppm: 4.29–4.34 (4H, m), 6.88 (1H, d, *J* = 8.2 Hz), 7.31–7.40 (3H, m), 7.52–7.58 (1H, q, *J* = 5.8 Hz), 7.67 (1H, s), 7.73 (1H, t, *J* = 7.3 Hz), 8.70 (1H, s), 10.55 (1H, s, NH); ¹³C NMR (DMSO-d₆, 75 MHz) δ/ppm: 66.3, 102.3, 111.7, 114.7, 114.9, 118.0, 118.8, 125.7, 126.5, 126.7, 131.5, 139.4, 142.0, 146.2, 158.4, 175.2; LC–MS (*m/z*): 313.3289 [MH⁺]. Anal. Calcd. for C₁₇H₁₃FN₂O₃: C, 65.38; H, 4.20; N, 8.97; found: C, 65.36; H, 4.23; N, 8.98.

(E)-5'-((4-fluorobenzylidene)amino)spiro[[1,3]dioxolane-2,3'-indolin]-2'-one (5l) Dark brown powder, 65% yield, mp. 206.5–207.9 °C; IR: 3281, 2982, 2901, 1746, 1706, 1630, 1480, 1197, 1168, 1132, 998, 831, 728, 609 cm⁻¹; ¹H NMR (DMSO-d₆, 300 MHz) δ/ppm: 4.26–4.31 (2H, m), 4.33–4.35 (2H, m), 6.87 (1H, d, *J* = 8.2 Hz), 7.27–7.37 (4H, m), 7.95–7.98 (2H, q, *J* = 5.9 Hz), 8.66 (1H, s), 10.53 (1H, s, NH); ¹³C NMR (DMSO-d₆, 75 MHz) δ/ppm: 66.3, 102.4, 111.7, 116.4, 116.7, 117.9, 126.4, 131.4, 131.5, 133.5, 141.7, 146.6, 158.5, 175.2; LC–MS (*m/z*): 313.2348 [MH⁺]. Anal. Calcd. for C₁₇H₁₃FN₂O₃: C, 65.38; H, 4.20; N, 8.97; found: C, 65.33; H, 4.24; N, 8.94.

(E)-5'-((2-chlorobenzylidene)amino)spiro[[1,3]dioxolane-2,3'-indolin]-2'-one (5m) Yellowish powder, 75.4% yield, mp. 271.5–273.3 °C; IR: 3148, 3106, 2967, 2904, 1700, 1627, 1478, 1274, 1200, 1073, 993, 755 cm⁻¹; ¹H NMR (DMSO-d₆, 300 MHz) δ/ppm: 4.30–4.33 (4H,

m), 6.89 (1H, d, $J=7.9$ Hz), 7.33–7.56 (5H, m), 8.13 (1H, d, $J=6.5$ Hz), 8.87 (1H, s), 10.58 (1H, s, NH); ^{13}C NMR (DMSO- d_6 , 75 MHz) δ/ppm : 66.3, 102.3, 111.9, 118.4, 118.6, 126.3, 126.5, 128.3, 128.9, 130.8, 133.4, 135.6, 142.2, 146.5, 155.3, 175.3; LC-MS (m/z): 351.1948 [MNa^+]. Anal. Calcd. for $\text{C}_{17}\text{H}_{13}\text{ClN}_2\text{O}_3$: C, 62.11; H, 3.99; N, 8.52; found: C, 62.15; H, 3.97; N, 8.54.

(E)-5'-((3-chlorobenzylidene)amino)spiro[[1,3]dioxolane-2,3'-indolin]-2'-one (5n) Brown powder, 74.3% yield, mp. 184.8–186.1 °C; IR: 3323, 2972, 2905, 1742, 1704, 1630, 1481, 1283, 1199, 1169, 1074, 1030, 781, 679 cm^{-1} ; ^1H NMR (DMSO- d_6 , 300 MHz) δ/ppm : 4.25–4.30 (2H, m), 4.32–4.37 (2H, m), 6.88 (1H, d, $J=8.2$ Hz), 7.31–7.34 (1H, dd, $J_1=2.0$ Hz, $J_2=8.2$ Hz), 7.40 (1H, d, $J=1.8$ Hz), 7.49–7.57 (2H, m), 7.85 (1H, d, $J=6.7$ Hz), 7.93 (1H, s), 8.68 (1H, s), 10.57 (1H, s, NH); ^{13}C NMR (DMSO- d_6 , 75 MHz) δ/ppm : 66.3, 102.3, 111.7, 118.1, 126.5, 126.6, 127.8, 128.4, 131.4, 131.5, 134.3, 138.9, 142.1, 146.2, 158.2, 175.2; LC-MS (m/z): 329.2433 [MH^+]. Anal. Calcd. for $\text{C}_{17}\text{H}_{13}\text{ClN}_2\text{O}_3$: C, 62.11; H, 3.99; N, 8.52; found: C, 62.14; H, 3.96; N, 8.55.

(E)-5'-((4-chlorobenzylidene)amino)spiro[[1,3]dioxolane-2,3'-indolin]-2'-one (5o) Brown powder, 75% yield, mp. 260.1–262.4 °C; IR: 3137, 3042, 2890, 2843, 1724, 1631, 1490, 1281, 1201, 1072, 993, 779, 607 cm^{-1} ; ^1H NMR (DMSO- d_6 , 300 MHz) δ/ppm : 4.28–4.34 (4H, m), 6.87 (1H, d, $J=8.2$ Hz), 7.31 (1H, d, $J=8.2$ Hz), 7.32 (1H, s), 7.56 (2H, d, $J=6.9$ Hz), 7.92 (2H, d, $J=6.9$ Hz), 8.68 (1H, s), 10.54 (1H, s, NH); ^{13}C NMR (DMSO- d_6 , 75 MHz) δ/ppm : 66.3, 102.3, 111.7, 118.0, 126.4, 126.5, 129.6, 130.8, 135.7, 136.5, 141.9, 146.4, 158.4, 175.2; LC-MS (m/z): 329.2477 [MH^+]. Anal. Calcd. for $\text{C}_{17}\text{H}_{13}\text{ClN}_2\text{O}_3$: C, 62.11; H, 3.99; N, 8.52; found: C, 62.13; H, 3.95; N, 8.56.

(E)-5'-((2-bromobenzylidene)amino)spiro[[1,3]dioxolane-2,3'-indolin]-2'-one (5p) Yellowish powder, 76% yield, mp. 216.9–218.2 °C; IR: 3178, 3106, 2968, 2902, 1728, 1627, 1476, 1271, 1201, 1072, 1028, 992, 754 cm^{-1} ; ^1H NMR (DMSO- d_6 , 300 MHz) δ/ppm : 4.28–4.40 (4H, m), 6.94 (1H, d, $J=7.9$ Hz), 7.34–7.38 (2H, m), 7.44–7.55 (2H, m), 7.75 (1H, d, $J=7.6$ Hz), 8.10–8.13 (1H, dd, $J_1=1.8$ Hz, $J_2=7.4$ Hz), 8.81 (1H, s), 10.64 (1H, s, NH); ^{13}C NMR (DMSO- d_6 , 75 MHz) δ/ppm : 66.3, 102.3, 111.9, 118.4, 125.9, 126.0, 126.5, 128.8, 129.4, 133.7, 133.9, 134.7, 142.2, 146.5, 157.7, 175.2; LC-MS (m/z): 397.0669 [MNa^+]. Anal. Calcd. for $\text{C}_{17}\text{H}_{13}\text{BrN}_2\text{O}_3$: C, 54.71; H, 3.51; N, 7.51; found: C, 54.76; H, 3.53; N, 7.48.

(E)-5'-((3-bromobenzylidene)amino)spiro[[1,3]dioxolane-2,3'-indolin]-2'-one (5q) Dark brown powder, 89% yield, mp. 271.9–272.9 °C; IR: 3322, 2969, 2901, 1741,

1704, 1629, 1480, 1210, 1168, 1070, 994, 821, 779 cm^{-1} ; ^1H NMR (DMSO- d_6 , 300 MHz) δ/ppm : 4.25–4.30 (2H, m), 4.32–4.37 (2H, m), 6.88 (1H, d, $J=8.2$ Hz), 7.31–7.34 (1H, dd, $J_1=2.3$ Hz, $J_2=8.2$ Hz), 7.40 (1H, d, $J=2.1$ Hz), 7.45 (1H, t, $J=7.9$ Hz), 7.69 (1H, d, $J=7.9$ Hz), 7.89 (1H, d, $J=8.0$ Hz), 8.08 (1H, s), 8.67 (1H, s), 10.57 (1H, s, NH); ^{13}C NMR (DMSO- d_6 , 75 MHz) δ/ppm : 66.3, 102.3, 111.7, 118.0, 122.8, 126.5, 126.7, 128.2, 131.4, 131.7, 134.4, 139.1, 142.0, 146.2, 158.1, 175.2; LC-MS (m/z): 375.1272 [MH^+]. Anal. Calcd. for $\text{C}_{17}\text{H}_{13}\text{BrN}_2\text{O}_3$: C, 54.71; H, 3.51; N, 7.51; found: C, 54.75; H, 3.54; N, 7.47.

(E)-5'-((4-bromobenzylidene)amino)spiro[[1,3]dioxolane-2,3'-indolin]-2'-one (5r) Orange powder, 60% yield, mp. 205.6–206.8 °C; IR: 3138, 3081, 3041, 2892, 1722, 1630, 1486, 1281, 1199, 1162, 1066, 992, 892, 778, 604 cm^{-1} ; ^1H NMR (DMSO- d_6 , 300 MHz) δ/ppm : 4.28–4.30 (2H, m), 4.32–4.38 (2H, m), 6.87 (1H, d, $J=8.2$ Hz), 7.29–7.32 (1H, dd, $J_1=2.1$ Hz, $J_2=8.2$ Hz), 7.39 (1H, d, $J=1.8$ Hz), 7.69 (2H, d, $J=8.5$ Hz), 7.83 (2H, d, $J=8.5$ Hz), 8.66 (1H, s), 10.55 (1H, s, NH); ^{13}C NMR (DMSO- d_6 , 75 MHz) δ/ppm : 66.3, 102.3, 111.7, 118.0, 125.4, 126.4, 126.5, 130.9, 132.5, 136.0, 141.9, 146.4, 158.5, 175.2; LC-MS (m/z): 375.1052 [MH^+]. Anal. Calcd. for $\text{C}_{17}\text{H}_{13}\text{BrN}_2\text{O}_3$: C, 54.71; H, 3.51; N, 7.51; found: C, 54.73; H, 3.55; N, 7.46.

(E)-5'-((2-nitrobenzylidene)amino)spiro[[1,3]dioxolane-2,3'-indolin]-2'-one (5s) Orange powder, 74% yield, mp. 258.8–260.0 °C; IR: 3140, 3101, 2970, 2900, 1720, 1622, 1516, 1481, 1344, 1216, 1169, 1068, 1027, 994, 733 cm^{-1} ; ^1H NMR (DMSO- d_6 , 300 MHz) δ/ppm : 4.25–4.31 (2H, m), 4.33–4.38 (2H, m), 6.90 (1H, d, $J=8.0$ Hz), 7.31–7.34 (1H, dd, $J_1=2.0$ Hz, $J_2=8.2$ Hz), 7.37 (1H, d, $J=2.0$ Hz), 7.70–7.76 (1H, td, $J_1=1.8$ Hz, $J_2=7.6$ Hz), 7.81–7.87 (1H, td, $J_1=1.0$ Hz, $J_2=7.6$ Hz), 8.06–8.09 (1H, dd, $J_1=1.2$ Hz, $J_2=8.2$ Hz), 8.12–8.15 (1H, dd, $J_1=1.2$ Hz, $J_2=8.0$ Hz), 8.89 (1H, s), 10.59 (1H, s, NH); ^{13}C NMR (DMSO- d_6 , 75 MHz) δ/ppm : 66.3, 102.3, 111.8, 118.3, 125.2, 126.4, 126.7, 130.1, 130.7, 132.3, 134.3, 142.5, 146.0, 149.9, 155.6, 175.2; LC-MS (m/z): 362.1700 [MNa^+]. Anal. Calcd. for $\text{C}_{17}\text{H}_{13}\text{N}_3\text{O}_5$: C, 60.18; H, 3.86; N, 12.38; found: C, 60.15; H, 3.83; N, 12.40.

(E)-5'-((3-nitrobenzylidene)amino)spiro[[1,3]dioxolane-2,3'-indolin]-2'-one (5t) Dark brown powder, 88.8% yield, mp. 214.3–216.0 °C; IR: 3174, 2963, 2897, 1735, 1622, 1524, 1476, 1348, 1199, 1072, 996, 813, 730, 613 cm^{-1} ; ^1H NMR (DMSO- d_6 , 300 MHz) δ/ppm : 4.29–4.32 (2H, m), 4.33–4.36 (2H, m), 6.90 (1H, d, $J=8.2$ Hz), 7.38 (1H, d, $J=8.2$ Hz), 7.47 (1H, s), 7.77 (1H, t, $J=7.0$ Hz), 8.30 (2H, d, $J=7.6$ Hz), 8.69 (1H, s), 8.85 (1H, s), 10.59 (1H, s, NH); ^{13}C NMR (DMSO- d_6 , 75 MHz) δ/ppm :

ppm: 66.3, 102.3, 111.8, 118.2, 123.1, 125.9, 126.5, 126.9, 131.1, 135.1, 138.4, 142.4, 145.8, 148.8, 157.5, 175.2; LC–MS (m/z): 340.25 [MH⁺]. Anal. Calcd. for C₁₇H₁₃N₃O₅: C, 60.18; H, 3.86; N, 12.38; found: C, 60.14; H, 3.84; N, 12.41.

(E)-5'-((4-nitrobenzylidene)amino)spiro[[1,3]dioxolane-2,3'-indolin]-2'-one (5u) Orange powder, 83.5% yield, mp. 268.8–270.4 °C; IR: 3286, 2963, 2898, 1748, 1709, 1632, 1512, 1485, 1338, 1198, 1165, 995, 845, 728, 605 cm⁻¹; ¹H NMR (DMSO-d₆, 300 MHz) δ /ppm: 4.25–4.30 (2H, m), 4.32–4.37 (2H, m), 6.89 (1H, d, J =8.2 Hz), 7.37–7.41 (1H, dd, J_1 =2.4 Hz, J_2 =8.2 Hz), 7.47 (1H, d, J =2.0 Hz), 8.13 (2H, d, J =8.8 Hz), 8.33 (2H, d, J =8.8 Hz), 8.85 (1H, s), 10.59 (1H, s, NH); ¹³C NMR (DMSO-d₆, 75 MHz) δ /ppm: 66.5, 102.5, 112.0, 118.3, 118.8, 124.9, 126.7, 127.4, 130.3, 142.6, 146.0, 149.5, 157.8, 175.4; LC–MS (m/z): 381.3993[MK⁺]. Anal. Calcd. for C₁₇H₁₃N₃O₅: C, 60.18; H, 3.86; N, 12.38; found: C, 60.16; H, 3.85; N, 12.37.

Antioxidant activity assays

In CUPRAC assay, the absorbance values were used to calculate the A_{0.50}, but in ABTS and DPPH assay, inhibition (%) values were used to calculate the IC₅₀.

DPPH (1,1-diphenyl-2-picrylhydrazyl) free radical scavenging assay

Free radical scavenging activities are determined using 1,1-diphenyl-2-picrylhydrazyl (DPPH) free radical [33]. 1000 μ M stock solutions of the materials were prepared. Of these stock solutions, 2, 5, 10 and 20 μ L was taken and completed to 40 μ L with ethanol, and then 160 μ L of 0.1 mM DPPH solution was added. The absorbance values of the prepared solutions were measured at 517 nm after 30 min of incubation in the dark at room temperature. Inhibition values (%) of the samples were calculated from the obtained absorbance values. The absorbance values of the samples were evaluated against the control.

ABTS cation radical decolourization assay

ABTS⁺ scavenging activities of the synthesized compounds were determined according to the literature method [34]. The solution of ABTS⁺ radical was generated by dissolving 19.2 mg of 2,2'-azino-bis(3-ethylbenzothiazoline-6-sulphonic acid) (7 mM ABTS) and 3.3 mg K₂S₂O₃ in distilled water (5 mL). The solution was kept in dark for 24 h at room temperature, and the absorbance of the solution was fixed to ~0.70 at 734 nm by dilution. The solutions of the samples were prepared in n-propanol at a

concentration of 1000 μ g/mL. The absorbance was measured at room temperature at 734 nm, after 6 min from ABTS⁺ addition. The decrease in the absorption was used for the calculation. The results were calculated as IC₅₀. Propyl alcohol was used as a solvent to controls.

Cupric reducing antioxidant capacity assay (CUPRAC)

Cupric reducing antioxidant capacities of the synthesized compounds were determined according to the literature method [35]. The solutions of compounds and standards were prepared in n-propanol at a concentration of 1000 μ g/mL. Different volumes (1000 mg/L and 54.5 mL) of the sample were added to a solution prepared by adding 61.0 μ L of 10 mM CuCl₂, 61.0 μ L of 7.5 mM neocuproine and 61.0 μ L of 1.0 mM NH₄CH₃COO buffer (pH = 7), respectively. The absorbance was measured at room temperature at 450 nm, after an hour. The results were calculated as A_{0.50}. Propyl alcohol was used as a solvent to controls.

Computational assay

Quantum chemical calculations were carried out by using the Q-CHEM 4.3, and the output files were visualized via IQmol program [43]. The optimized molecular structures of compounds in the ground states were obtained at the B3LYP/6-311G(d,p) [44] level of density functional theory (DFT). Afterwards, the FMOs (the frontier molecular orbitals: HOMO and LUMO called highest occupied and lowest unoccupied molecular orbitals) calculations were performed at the same level. Finally, the chemical hardness (η), softness (S) and electronegativity (χ) parameters associated with FMO energies were obtained by using same level. The calculation of FMO energies and related parameters (the electronegativity (χ), chemical hardness (η) and softness (S) parameters) for compounds was performed by using B3LYP/6-311G(d,p) level. The χ , η and S parameters were obtained by using $\chi = (IP + EA)/2$, $\eta = (IP - EA)/2$ and $S = 1/\eta$ equations [45].

Acknowledgements This work was supported by the Sakarya Research Fund of the Sakarya University (Project Number: 2014-50-01-036).

Compliance with ethical standards

Conflict of interest The authors declare they have no conflict of interest.

References

- Pisoschi AM, Pop A (2015) The role of antioxidants in the chemistry of oxidative stress: a review. *Eur J Med Chem* 97:55–74. <https://doi.org/10.1016/j.ejmech.2015.04.040>
- Lozynskiy A, Zasadko V et al (2017) Synthesis, antioxidant and antimicrobial activities of novel thiopyrano[2,3-d]thiazoles based on acryloyl acrylic acids. *Mol Divers* 21:427–436. <https://doi.org/10.1007/s11030-017-9737-8>
- Dai Y, Shao C et al (2017) The mechanism for cleavage of three typical glucosidic bonds induced by hydroxyl free radical. *Carbohydr Polym* 178:34–40. <https://doi.org/10.1016/j.carbpol.2017.09.016>
- Mason RP (2016) Imaging free radicals in organelles, cells, tissue, and in vivo with immuno-spin trapping. *Redox Biol* 8:422–429. <https://doi.org/10.1016/j.redox.2016.04.003>
- Trinity JD, Broxterman RM, Richardson RS (2016) Regulation of exercise blood flow: role of free radicals. *Free Radic Biol Med* 98:90–102. <https://doi.org/10.1016/j.freeradbiomed.2016.01.017>
- Razzaq H, Saira F et al (2016) Interaction of gold nanoparticles with free radicals and their role in enhancing the scavenging activity of ascorbic acid. *J Photochem Photobiol, B* 161:266–272. <https://doi.org/10.1016/j.jphotobiol.2016.04.003>
- Si W, Chen YP et al (2018) Antioxidant activities of ginger extract and its constituents toward lipids. *Food Chem* 239:1117–1125. <https://doi.org/10.1016/j.foodchem.2017.07.055>
- Bentz EN, Pomilio AB, Lobayan RM (2017) Donor-acceptor interactions as descriptors of the free radical scavenging ability of flavans and catechin. *Comput Theor Chem* 1110:14–24. <https://doi.org/10.1016/j.comptc.2017.03.028>
- Komeri R, Thankam FG, Muthu J (2017) Free radical scavenging injectable hydrogels for regenerative therapy. *Mater Sci Eng C-Mater* 71:100–110. <https://doi.org/10.1016/j.msec.2016.09.087>
- Sridharan M, Prasad KJR et al (2016) Application of UV-Vis spectrophotometric process for the assessment of indoloacridines as free radical scavenger. *J Photochem Photobiol, B* 162:641–645. <https://doi.org/10.1016/j.jphotobiol.2016.07.026>
- Sivaguru P, Parameswaran K, Lalitha A (2017) Antioxidant, anticancer and electrochemical redox properties of new bis(2,3-dihydroquinazolin-4(1H)-one) derivatives. *Mol Divers* 21:611–620. <https://doi.org/10.1007/s11030-017-9748-5>
- Giorno TBS, Silva BVD et al (2016) Antinociceptive effect and mechanism of action of isatin, N-methyl isatin and oxopropyl isatin in mice. *Life Sci* 151:189–198. <https://doi.org/10.1016/j.lfs.2016.02.052>
- Ugale V, Patel H et al (2017) Benzofurano-isatins: search for antimicrobial agents. *Arab J Chem* 10:S389–S396. <https://doi.org/10.1016/j.arabjc.2012.09.011>
- Pavlovskaya TL, Redkin RG et al (2016) Molecular diversity of spirooxindoles. Synthesis and biological activity. *Mol Divers* 20:299–344. <https://doi.org/10.1007/s11030-015-9629-8>
- Gazieva GA, Izmestev AN et al (2018) The influence of substituents on the reactivity and cytotoxicity of imidazothiazolotriazinones. *Mol Divers* 22:585–589. <https://doi.org/10.1007/s11030-018-9813-8>
- Justo LA, Duran R et al (2016) Effects and mechanism of action of isatin, a MAO inhibitor, on in vivo striatal dopamine release. *Neurochem Int* 99:147–157. <https://doi.org/10.1016/j.neuint.2016.06.012>
- Xu Z, Zhang S et al (2017) Design, synthesis and in vitro antimycobacterial evaluation of gatifloxacin-1H-1,2,3-triazole-isatin hybrids. *Bioorg Med Chem Lett* 27(16):3643–3646. <https://doi.org/10.1016/j.bmcl.2017.07.023>
- Wang G, Chen M et al (2018) Synthesis, in vitro alpha-glucosidase inhibitory activity and docking studies of novel chromone-isatin derivatives. *Bioorg Med Chem Lett* 28(2):113–116. <https://doi.org/10.1016/j.bmcl.2017.11.047>
- Singh H, Singh JV et al (2017) Triazole tethered isatin-coumarin based molecular hybrids as novel antitubulin agents: design, synthesis, biological investigation and docking studies. *Bioorg Med Chem Lett* 27(17):3974–3979. <https://doi.org/10.1016/j.bmcl.2017.07.069>
- Ibrahim HS, Abou-seri SM et al (2016) Bis-isatin hydrazones with novel linkers: synthesis and biological evaluation as cytotoxic agents. *Eur J Med Chem* 108:415–422. <https://doi.org/10.1016/j.ejmech.2015.11.047>
- Wang J, Yun D et al (2017) Design, synthesis and QSAR study of novel isatin analogues inspired Michael acceptor as potential anticancer compounds. *Eur J Med Chem* 144:493–503. <https://doi.org/10.1016/j.ejmech.2017.12.043>
- Kausar N, Masum AA et al (2017) A green synthetic approach toward the synthesis of structurally diverse spirooxindole derivative libraries under catalyst-free conditions. *Mol Divers* 21:325–337. <https://doi.org/10.1007/s11030-017-9728-9>
- Andreani A, Burnelli S et al (2010) New isatin derivatives with antioxidant activity. *Eur J Med Chem* 45:1374–1378. <https://doi.org/10.1016/j.ejmech.2009.12.035>
- Lucarini M, Pedrielli P et al (1999) Bond dissociation energies of the N–H bond and rate constants for the reaction with alkyl, alkoxy, and peroxy radicals of phenothiazines and related compounds. *J Am Chem Soc* 121:11546–11553. <https://doi.org/10.1021/ja992904u>
- Pakravan P, Kashanian S et al (2013) Biochemical and pharmacological characterization of isatin and its derivatives: from structure to activity. *Pharmacol Rep* 65:313–335. [https://doi.org/10.1016/S1734-1140\(13\)71007-7](https://doi.org/10.1016/S1734-1140(13)71007-7)
- Visagaperumal D, Ezekwem JE et al (2018) Isatin schiff base-an overview. *PharmaTutor* 6:38–47. <https://doi.org/10.29161/PT.v6.i5.2018.38>
- Ghosh S, Roy N et al (2018) Photophysics of a coumarin based schiff base in solvents of varying polarities. *Spectrochim Acta A* 188:252–257. <https://doi.org/10.1016/j.saa.2017.07.006>
- Xia L, Xia YF et al (2015) Benzaldehyde Schiff bases regulation to the metabolism, hemolysis, and virulence genes expression in vitro and their structure-microbicidal activity relationship. *Eur J Med Chem* 97:83–93. <https://doi.org/10.1016/j.ejmech.2015.04.042>
- Gencer N, Sonmez F et al (2014) Synthesis, structure-activity relationships and biological activity of new isatin derivatives as tyrosinase inhibitors. *Curr Top Med Chem* 14(12):1450–1462. <https://doi.org/10.2174/1568026614666140530104344>
- Huong TTL, Dung DTM et al (2015) Novel 2-oxoindoline-based hydroxamic acids: synthesis, cytotoxicity, and inhibition of histone deacetylation. *Tetrahedron Lett* 56(46):6425–6429. <https://doi.org/10.1016/j.tetlet.2015.09.147>
- Wang X, Yin J et al (2014) Design, synthesis, and antibacterial activity of novel Schiff base derivatives of quinazolin-4(3H)-one. *Eur J Med Chem* 77:65–74. <https://doi.org/10.1016/j.ejmech.2014.02.053>
- Floegel A, Kim DO et al (2011) Comparison of ABTS/DPPH assays to measure antioxidant capacity in popular antioxidant-rich US foods. *J Food Compos Anal* 24:1043–1048. <https://doi.org/10.1016/j.jfca.2011.01.008>
- Kedare SB, Singh RP (2011) Genesis and development of DPPH method of antioxidant assay. *J Food Sci Technol* 48(4):412–422. <https://doi.org/10.1007/s13197-011-0251-1>
- Kurt BZ, Gazioglu I et al (2015) Synthesis, antioxidant and anticholinesterase activities of novel coumarylthiazole derivatives. *Bioorg Chem* 59:80–90. <https://doi.org/10.1016/j.bioorg.2015.02.002>

35. Kurt BZ, Gazioglu I et al (2015) Potential of aryl-urea-benzofuranylthiazoles hybrids as multitasking agents in Alzheimer's disease. *Eur J Med Chem* 102:80–92. <https://doi.org/10.1016/j.ejmech.2015.07.005>
36. Belkheiri N, Bouguerne B et al (2010) Synthesis and antioxidant activity evaluation of a syringic hydrazones family. *Eur J Med Chem* 45:3019–3026. <https://doi.org/10.1016/j.ejmech.2010.03.031>
37. Apak R, Ozyurek M et al (2016) Antioxidant activity/capacity measurement. 1. Classification, physicochemical principles, mechanisms, and electron transfer (ET)-based assays. *J Agric Food Chem* 64:997–1027. <https://doi.org/10.1021/acs.jafc.5b04739>
38. Powis G (1989) Free radical formation by antitumor quinones. *Free Radic Biol Med* 6:63–101. [https://doi.org/10.1016/0891-5849\(89\)90162-7](https://doi.org/10.1016/0891-5849(89)90162-7)
39. Soares MA, Lessa JA et al (2012) N⁴-Phenyl-substituted 2-acetylpyridine thiosemicarbazones: cytotoxicity against human tumor cells, structure–activity relationship studies and investigation on the mechanism of action. *Bioorg Med Chem* 20:3396–3409. <https://doi.org/10.1016/j.bmc.2012.04.027>
40. Atahan A, Gencer N et al (2018) Synthesis, biological activity and structure-activity relationship of novel diphenylurea derivatives containing tetrahydroquinoline as carbonic anhydrase I and II inhibitors. *ChemistrySelect* 3:529–534. <https://doi.org/10.1002/slct.201702562>
41. Minkin VI (1999) Glossary of terms used in theoretical organic chemistry. *Pure Appl Chem* 71:1919. <https://doi.org/10.1351/pac199971101919>
42. Ho TL (1975) The hard soft acids bases (HSAB) principle and organic chemistry. *Chem Rev* 75:1–20. <https://doi.org/10.1021/cr60293a001>
43. Shao Y, Gan Z et al (2015) Advances in molecular quantum chemistry contained in the Q-Chem 4 program package. *Mol Phys* 113(2):184–215. <https://doi.org/10.1080/00268976.2014.952696>
44. Becke AD (1993) A new mixing of Hartree-Fock and local density-functional theories. *J Chem Phys* 98:1372–1377. <https://doi.org/10.1063/1.464304>
45. Altürk S, Avcı D et al (2016) A cobalt (II) complex with 6-methylpicolinate: synthesis, characterization, second- and third-order nonlinear optical properties, and DFT calculations. *J Phys Chem Solids* 98:71–80. <https://doi.org/10.1016/j.jpcs.2016.06.008>

Publisher's Note Springer Nature remains neutral with regard to jurisdictional claims in published maps and institutional affiliations.